isvr Institute of Sound and Vibration Research

Active Vibration Control of a Railway Pantograph

T.X. Wu and M.J. Brennan

ISVR Technical Memorandum 820

June 1997

University of Southampton

SCIENTIFIC PUBLICATIONS BY THE ISVR

Technical Reports are published to promote timely dissemination of research results by ISVR personnel. This medium permits more detailed presentation than is usually acceptable for scientific journals. Responsibility for both the content and any opinions expressed rests entirely with the author(s).

Technical Memoranda are produced to enable the early or preliminary release of information by ISVR personnel where such release is deemed to the appropriate. Information contained in these memoranda may be incomplete, or form part of a continuing programme; this should be borne in mind when using or quoting from these documents.

Contract Reports are produced to record the results of scientific work carried out for sponsors, under contract. The ISVR treats these reports as confidential to sponsors and does not make them available for general circulation. Individual sponsors may, however, authorize subsequent release of the material.

UNIVERSITY OF SOUTHAMPTON

INSTITUTE OF SOUND AND VIBRATION RESEARCH

STRUCTURAL DYNAMICS GROUP

Active Vibration Control of a Railway Pantograph

by

T.X. Wu and M.J. Brennan

ISVR Technical Memorandum No. 820

June 1997

Authorized for issue by
Dr. R.J. Pinnington
Group Chairman

TABLE OF CONTENTS

LIST OF FIGURES

Abstract

Current collection for electrical trains can be improved by the use of an active pantograph. To design such a system the behaviour of both the active pantograph and the overhead catenary system must be considered together. In this paper a two degrees of freedom model of an active pantograph, combined with a time-varying spring representing the catenary's influence is employed, and its dynamic performance is studied. Based on this model, three types of control strategies for an active pantograph are proposed and investigated, and all these models consider the interaction of the pantograph with the overhead wire. Two possible positions for mounting an actuator on the pantograph are considered and compared. From these active pantograph models the magnitude of the control force required can be estimated, and the advantages and disadvantages are discussed. The optimal control strategy shows the best performance, but introduces measurement difficulties because it needs full-state feedback. Classical feedback control is the least difficult to implement, but a compromise between the stability and the performance should be reached.

1 Introduction

For a high speed electrical train one of the key operations is current collection. This task is accomplished by a pantograph mounted on the roof of the locomotive and an overhead wire system. When the train operates, the pantograph head is in contact with the overhead wire and electric power is transferred to the train. Unfortunately, as the operational speed of a train increases, the vibration of the pantograph and the overhead wire also increases. It may lead to a zero contact force between the pantograph head (panhead) and the overhead wire, and therefore, loss of contact, arcing and wear.

The pantograph and the overhead wire is a dynamic coupled system. They affect each other through the contact force. A main source of vibration is the stiffness variation of the overhead wire along the span [1]. In the middle of a span the stiffness of the overhead wire is minimum and near the support tower it is maximum. When the pantograph moves along the overhead wire, its stiffness variation produces a periodic excitation which leads to vibration of the pantograph and fluctuation of the contact force. Additionally, as the panhead moves along the overhead wire it causes a flexural wave motion in the wire. In turn, this flexural wave propagation also affects the contact force and the motion of the pantograph.

The dynamic interaction of the pantograph and the catenary has been studied extensively over the years. An approximate analytical solution for the contact force has been presented by Ockendon et al. [2]. Vinayagaligam [3] studied the contact force variation and the panhead trajectory by using the finite difference methods. Wormley et al. [4] obtained the free vibration modes of the overhead wire system and the contact force by using the Rayleigh-Ritz and model analysis methods respectively. Wu [5] developed a finite element model of the pantograph-catenary system to study the current collection problem by numerical simulation. Yagi et al. [6] investigated the dynamic response of the pantograph-catenary system to the lateral movement of the overhead wire due to its zigzag layout.

In general, for a passive pantograph there are probably two possible ways to avoid the loss of contact between the panhead and the overhead wire at higher train speeds. One is to reduce the mass of a pantograph, and the other is to reduce the stiffness fluctuation and increase the average stiffness of an overhead wire. The latter means the use of a compound catenary system which has high construction and maintenance costs. Even if these methods are used, the improvement in the dynamic performance of the pantograph-catenary system is limited. An alternative approach to solving the problem is to use an active pantograph. This permits the use of a less complex and hence less expensive catenary system or a higher operational train speed for a given catenary system.

Some work has been conducted on active pantograph systems. An active pantograph using a hydraulic servo has been proposed by Vinayagalingam [7], and Galeotti et al. [8] have investigated some active pantograph models that use linear force motors. Huber et al. [9] described some control strategies using a multiple degrees of freedom pantograph model and several different models of the catenary. Thompson and Davis [10] employed an optimal controller using an incomplete state feedback for an active pantograph with the goal of minimising its mechanical impedance in the low frequency range.

The active pantograph models cited above mainly use closed-loop feedback control, in which it is difficult to keep the contact force constant. This is due to the compromise between the stability and the performance of a feedback control system. For an active pantograph different control strategies will lead to different results in both performance and stability. In addition, there is more than one position to mount an actuator for an active pantograph. An appropriate position for the actuator should be decided by considering the following aspects (i) the magnitude of the control force required, (ii) the convenience of mounting an actuator and (iii) the influence of the actuator on the dynamic performance of the pantograph. The aim of this paper is to study these aspects comprehensively using a simple model of the pantograph-catenary system.

A two DOF active pantograph model combined with a time-varying spring representing the catenary's influence is employed, and its dynamic performance is studied. Based on this model, open-loop, feedback and optimal control strategies with the aim of maintaining a constant contact force are proposed and investigated, and two possible positions for mounting an actuator are compared. From these studies the control force required can be estimated, and the advantages and disadvantages of various control strategies and actuator positions are discussed. For simplicity some factors such as initial sag of the overhead wire, fundamental excitation of the locomotive roof and aerodynamic force to the pantograph are not included in these models.

2 Passive Pantograph and Catenary System

A picture of a real pantograph-catenary system is shown in Fig. 1 and a much simplified two DOF dynamic model of the pantograph is shown in Fig. 2. M_1 and M_2 represent the equivalent masses of the panhead and the frame of a pantograph respectively, K_1 is the stiffness of the panhead suspension, and C_1 and C_2 are the viscous damping coefficients of the pantograph suspension and the frame to the ground respectively. F_C represents the contact force between the catenary and the pantograph, and F_L the static uplift force applied to the pantograph.

The stiffness variation of the overhead wire in a span is a primary source of the vibration of the pantograph. A standard catenary system and the static stiffness of a typical overhead wire are shown in Fig. 3 and these are taken from reference [1]. If wave propagation in the wire is considered, dynamic rather than static stiffness should be used. The dynamic stiffness of an overhead wire varies with the tension, the density of the wire and the speed of the pantograph. Compared to the static stiffness, the dynamic stiffness will dramatically change when the speed of the pantograph is close to the wave speed in the wire, which is constant at about 400 km/h, but it is very similar to the static stiffness if the moving speed is below eighty percent of the wave speed [11]. For simplicity only the static stiffness of the overhead wire is used in this

paper, and a pantograph-catenary model including static stiffness variation of the catenary K(t) is shown in Fig. 4. If the high frequency component of the stiffness fluctuation between the droppers is neglected, the time-varying stiffness K(t) can be written as

$$K(t) = K_0(1 + \alpha \cos\frac{2\pi V}{L} t) \tag{1a}$$

where

$$K_0 = \frac{1}{2}(K_{\max} + K_{\min}) \tag{1b}$$

and

$$\alpha = \frac{K_{\max} - K_{\min}}{K_{\max} + K_{\min}} \tag{1c}$$

where K_{max} and K_{min} are the maximum and minimum stiffness of the overhead wire in a span respectively. K_0 is the average stiffness and α is the stiffness variation coefficient in a span. For different overhead wire systems α typically varies from 0.3 to 0.6. V is the operational speed of a train, and L is the span length.

Based on the assumptions above, the equations of motion of the pantograph-catenary system model shown in Fig. 4 can be written as

$$M_1\ddot{x}_1 + C_1(\dot{x}_1 - \dot{x}_2) + K_1(x_1 - x_2) + K(t)x_1 = 0 \tag{2a}$$

$$M_2\ddot{x}_2 + C_1(\dot{x}_2 - \dot{x}_1) + C_2\dot{x}_2 + K_1(x_2 - x_1) = F_L \tag{2b}$$

The contact force F_C is given by

$$F_C = K_1(t)x_1 \tag{3}$$

and a loss of contact between the pantograph and the catenary will occur when F_C has a negative value.

Equations (2a,b) represent a parametrically excited system, so the stability of the solutions should be examined first. Wu and Brennan [1] considered this for the system discussed in this paper and showed that a practical pantograph-catenary system is generally stable, and that the loss of contact at higher speeds is probably caused by the normal (bounded) vibration of the system.

For a numerical solution to equations (2) and (3) the following parameters are employed:

M_1=8kg	M_2=12kg	K_1=10kN/m
C_1=120Ns/m	C_2=30Ns/m	K_0=3.6kN/m
α=0.5	L=65m	F_L=100N

The numerical simulation results for the panhead displacement and the contact force are obtained by using the 4th order Runge-Kutta method. Fig. 5 shows the displacement and the contact force in the form of peak-to-peak and maximum values at different operational speeds.

From Fig. 5 it can be seen that there are three main peaks of the panhead displacement and the contact force. Setting

$$\omega_n = \sqrt{K_0/(M_1 + M_2)} \quad \text{and} \quad \omega = 2\pi V / L,$$

where ω_n can be regarded as the nominally natural frequency of the pantograph-catenary system and ω is the stiffness variation frequency which is related to the train's operational speed and the span length, then we can estimate that these peaks appear at approximately $\omega=\omega_n/3$, $\omega=\omega_n/2$, and $\omega=\omega_n$ [1]. *If the peak-to-peak displacement or contact force is greater than the maximum displacement or contact force respectively, the loss of contact between the panhead and the overhead wire will occur*. Therefore, the first crossing point of the peak-to-peak and the maximum graphs represents the limit of the operational speed of a train. For a pantograph-catenary system having the parameters detailed above, the maximum speed is about 150 km/h. When a secure margin of positive contact force is considered, the practical maximum speed may be only 130 km/h.

It should be pointed out that if the wave propagation in the overhead wire is considered, the results will become worse than those shown in Fig. 5 when the speed of trains is greater than 320 km/h. This is because the dynamic stiffness fluctuation

will become larger than the static stiffness fluctuation when the speed of a train is close to the wave speed in the overhead wire.

For a passive pantograph the only way to avoid the loss of contact at higher speed is to reduce both the head mass and the frame mass of the pantograph, but this is limited by the required current-carrying capacity of the pantograph.

3 An Active Pantograph

In this section three types of control strategies for an active pantograph are discussed. All these models consider the interaction of the pantograph with the overhead wire which is modelled as a time-varying stiffness as discussed above.

3.1 Open-Loop Control

For an active pantograph there are two convenient positions to mount an actuator. One is between the panhead and the frame, the other between the frame and the base of the pantograph. By considering open-loop control the magnitude of the secondary force can be established without considering the problems of closed-loop stability. Fig. 6 shows the case, where the secondary force F_S acts between the panhead and the frame, and the equations of motion of this system can be written as

$$M_1\ddot{x}_1 + C_1(\dot{x}_1 - \dot{x}_2) + K_1(x_1 - x_2) + K(t)x_1 = F_S \tag{4a}$$

$$M_2\ddot{x}_2 + C_1(\dot{x}_2 - \dot{x}_1) + C_2\dot{x}_2 + K_1(x_2 - x_1) = F_L - F_S \tag{4b}$$

The goal of active control is to keep the contact force F_C constant, that is

$$F_C = K(t)x_1 = const. \tag{5}$$

Now, the panhead displacement x_1 can be determined by combining equations (1a) and (3) to give

$$x_1 = \frac{F_C}{K(t)} = \frac{F_C}{K_0(1+\alpha\cos\frac{2\pi V}{L}t)} \tag{6}$$

and x_1 can be expressed in terms of the Fourier series as

$$x_1 = \frac{F_C}{K_0}\frac{1}{1+\alpha\cos\frac{2\pi V}{L}t} = \frac{F_C}{K_0}\sum_{i=0}^{\infty} a_i \cos\omega_i t \tag{7a}$$

where

$$a_i = \frac{1}{\sqrt{1-\alpha^2}}, \quad i=0; \quad a_i = \frac{2\left(\sqrt{1-\alpha^2}-1\right)^i}{\alpha^i\sqrt{1-\alpha^2}}, \quad i \geq 0 \tag{7b}$$

$$\omega_i = \frac{2\pi V i}{L} \tag{7c}$$

We can thus write the displacements of the panhead and the frame x_1 and x_2 respectively as a sum of their DC (or static components) x_{10} and x_{20} and their dynamic components, which gives

$$x_1 = x_{10} + \sum_{i=1}^{\infty} x_{1i}(t) = \frac{F_C}{K_0}(a_0 + \sum_{i=1}^{\infty} a_i \cos\omega_i t) \tag{8a}$$

$$x_2 = x_{20} + \sum_{i=1}^{\infty} x_{2i}(t) \tag{8b}$$

The secondary force can also be written in terms of its Fourier components as

$$F_S = \sum_{i=1}^{\infty} f_{si}(t) \tag{8c}$$

Substituting (5) and (8) into (4) and separating the equations into static and dynamic sets, then we have

$$K_1(x_{10} - x_{20}) = -F_C \tag{9a}$$

$$K_1(x_{20} - x_{10}) = F_L \tag{9b}$$

and

$$M_1\ddot{x}_{1i} + C_1(\dot{x}_{1i} - \dot{x}_{2i}) + K_1(x_{1i} - x_{2i}) = f_{si} \tag{10a}$$

$$M_2\ddot{x}_{2i} + C_1(\dot{x}_{2i} - \dot{x}_{1i}) + C_2\dot{x}_{2i} + K_1(x_{2i} - x_{1i}) = -f_{si} \tag{10b}$$

$$i = 1,2,\cdots,\infty$$

Equation (9) yields

$$F_C = F_L = const.$$

x_{1i} can be determined from equations (7a,b,c) and then, f_{si} and x_{2i} can be derived using equations (10a,b). We can write the complex form of x_{1i}, x_{2i} and f_{si} as

$$x_{1i} = X_{1i}e^{j\omega_i t} \tag{11a}$$

$$x_{2i} = X_{2i}e^{j\omega_i t} \tag{11b}$$

$$f_{si} = F_{si}e^{j\omega_i t} \tag{11c}$$

where X_{1i}, X_{2i} and F_{si} are complex amplitudes, and substitute (11) into (10) to give

$$(K_1 - \omega_i^2 M_1 + j\omega_i C_1)X_{1i} = (K_1 + j\omega_i C_1)X_{2i} + F_{si} \tag{12a}$$

$$[K_1 - \omega_i^2 M_2 + j\omega_i (C_1 + C_2)]X_{2i} = (K_1 + j\omega_i C_1)X_{1i} - F_{si} \tag{12b}$$

It can be seen from (12) that the required active control force F_S to maintain a constant contact force is a function of the panhead displacement x_1. We can obtain F_S by combining equations (8), (11) and (12) to give

$$F_S = F_C \frac{K_1}{K_0} \sum_{i=1}^{\infty} a_i [\sqrt{(1 - \omega_i^2 M_1/K_1)^2 + (\omega_i C_1/K_1)^2}\cos(\omega_i t + \varphi_{1i})$$

$$+\omega_i M_1 \sqrt{\frac{1 + (\omega_i C_1/K_1)^2}{(\omega_i M_2)^2 + C_2^2}}\cos(\omega_i t + \varphi_{2i})] \tag{13a}$$

where

$$\varphi_{1i} = \tan^{-1}\frac{\omega_i C_1}{K_1 - \omega_i^2 M_1} \tag{13b}$$

and

$$\varphi_{2i} = \tan^{-1}\frac{\omega_i C_1}{K_1} + \tan^{-1}\frac{C_2}{\omega_i M_2} \tag{13c}$$

where a_i and ω_i can be calculated using (7b) and (7c) respectively.

It can be seen from (13), the active control force F_S is proportional to the stiffness of the panhead suspension. If K_1 is stiff, a large F_S is required and vice versa. Therefore,

when the actuator is placed between the panhead and the frame, a softer panhead suspension is beneficial, as it reduces the secondary force required. Fig. 7 shows the results of the open-loop control of the active pantograph which has the same parameters as the passive pantograph discussed above. In general, it is sufficient to take only the first three terms in (13) to obtain a satisfactory approximate solution.

In practice, the panhead-frame mounted actuator would have the disadvantage of increasing the panhead mass. This would lead to a poor dynamic performance of the pantograph so that a larger active control force would be required. The frame actuated active pantograph may be more acceptable. Many pantographs have a pneumatic cylinder on the base to provide the uplift force and it may be possible to modify it for active control.

Fig. 8 shows the frame actuated active pantograph model, and the equations of motion can be written as

$$M_1\ddot{x}_1 + C_1(\dot{x}_1 - \dot{x}_2) + K_1(x_1 - x_2) + K(t)x_1 = 0 \tag{14a}$$

$$M_2\ddot{x}_2 + C_1(\dot{x}_2 - \dot{x}_1) + C_2\dot{x}_2 + K_1(x_2 - x_1) = F_L + F_S \tag{14b}$$

Applying the same procedure to (14) as to (4), we obtain the following results

$$F_C = F_L = const.$$

$$F_S = \frac{F_C}{K_0}\sum_{i=1}^{\infty} a_i\omega_i[\sqrt{\omega_i^{\,2}(M_1+M_2)^2 + C_2^{\,2}}\cos(\omega_i t + \varphi_{1i}) + \omega_i^{\,2}\sqrt{\frac{(\omega_i M_1 M_2)^2 + (M_1 C_2)^2}{K_1^{\,2} + (\omega_i C_1)^2}}\cos(\omega_i t + \varphi_{2i})] \tag{15a}$$

$$\varphi_{1i} = \pi - \tan^{-1}\frac{C_1}{\omega_i(M_1+M_2)} \tag{15b}$$

$$\varphi_{2i} = -\tan^{-1}\frac{C_2}{\omega_i M_2} - \tan^{-1}\frac{\omega_i C_1}{K_1} \tag{15c}$$

It can be seen from (15) that the active control force required increases when the operational speed of trains increases. Fig. 9 shows the results of the frame actuated

active pantograph with the same parameters as the passive pantograph discussed above. From Fig. 9 it can be seen that the active control force F_S is quite small, compared with the panhead-frame actuated active pantograph. It is only about 130 N maximum for a 100 N contact force at the speed of 300 km/h. This means that the capacity of the pneumatic actuator would only need to be increased by about thirty percent if it were to be used to generate the secondary force.

This analysis of an open-loop control strategy has enabled the secondary force to be calculated for two different practical actuator configurations. However, a realistic control system would require a closed-loop control strategy and this is discussed in the next section.

3.2 Feedback Control

The isolated diagram of a frame actuated active pantograph is shown in Fig. 10 where K(t) and C_2 are replaced by the contact force F_C and the damping force $C_2\dot{x}_2$ respectively. The equilibrium equation can be written as

$$M_1\ddot{x}_1 + M_2\ddot{x}_2 + C_2\dot{x}_2 = F_S + F_L - F_C \tag{16}$$

If the control force is determined by

$$F_S = M_1\dot{x}_1 + M_2\ddot{x}_2 + C_2\dot{x}_2 \tag{17}$$

then

$$F_C = F_L = const.$$

Therefore, the active control force F_S can be produced through acceleration and velocity feedback.

Considering the stability of a feedback control system, (17) cannot be directly used for producing the control force because it represents the critical state between stability and instability. A compromise between the performance and the stability for a feedback control system should be reached, so the practical control force should be produced through

$$F_S = g_1 M_1 \ddot{x}_1 + g_2 M_2 \ddot{x}_2 + g_3 C_2 \dot{x}_2 \tag{18}$$

where g_1, g_2 and g_3 are the feedback coefficients, and satisfy the relationship

$$0 < g_1, g_2, g_3 < 1 \tag{19}$$

In this case, the contact force F_C will no longer be constant. Its fluctuation is related to the feedback coefficients g_1, g_2 and g_3. Substituting (18) into (16) yields

$$F_C = F_L - (1-g_1)M_1\ddot{x}_1 - (1-g_2)M_2\ddot{x}_2 - (1-g_3)C_2\dot{x}_2 \tag{20}$$

From (20) it can be seen that if g_1, g_2 and g_3 are close to 1, the fluctuation of the contact force will be small, but the margin of the stability will also be small, so a compromise should be considered.

Furthermore, if the whole system, that is the active pantograph combined with the overhead wire, is taken into account, the stability problem of the system will be more complicated. The equations of motion of the pantograph-catenary system with the active control force using acceleration and velocity feedback can be written as

$$M_1\ddot{x}_1 + C_1(\dot{x}_1 - \dot{x}_2) + K_1(x_1 - x_2) + K(t)x_1 = 0 \tag{21a}$$

$$(1-g_2)M_2\ddot{x}_2 - g_1M_1\ddot{x}_1 + C_1(\dot{x}_2 - \dot{x}_1) + (C_2 - g_3)\dot{x}_2 + K_1(x_2 - x_1) = F_L \tag{21b}$$

where

$$K(t) = K_0(1 + \alpha\cos\frac{2\pi V}{L}t)$$

Equations (21) still represent a parametrically excited system, but now there is a control force. The boundaries of the stable and unstable areas of the solution depend on the parameters of the pantograph-catenary system and also on the feedback coefficients g_1, g_2 and g_3. This makes it much more difficult to determine the boundaries between stability and instability.

In practice, it is unnecessary to investigate the stability of the system separately when the numerical calculations are carried out. If a numerical solution is divergent, it will be clear that the system is unstable, and so these proposed feedback coefficients will not be acceptable.

Fig. 11 and Fig. 12 show situations of an active pantograph using feedback control. For simplicity, g_1 and g_2 have the same value, and the parameters of the pantograph are the same as before. From Fig. 11 and Fig. 12 some important points of the active pantograph using acceleration and velocity feedback control may be summarised, they are:

1. The goal of keeping the contact force constant cannot be achieved because there is a compromise between the performance and the stability for a feedback control system.

2. The velocity feedback g_3 is not always beneficial because it reduces the damping which is important to keep the system stable.

3. The larger the stiffness of the panhead suspension, the better the results.

Another very useful point is that acceleration feed back control has the advantage of avoiding measurement problems since accurate measurement of displacements and velocities can be difficult to achieve directly and accelerometers readily provide reliable measurement of accelerations.

3.3 Optimal Feedback Control

Because it is difficult to maintain a constant contact force using classical feedback control, another way to achieve the goal of keeping the contact force constant could be to use optimal feedback control.

For optimal control the equation of motion of the pantograph-catenary system should be represented in state-space form [12], which is

$$\boldsymbol{X}(t) = \boldsymbol{A}(t)\boldsymbol{X}(t) + \boldsymbol{B}\boldsymbol{U}(t) \tag{21}$$

where

$$\boldsymbol{X}(t) = \begin{bmatrix} x_1 & x_2 & \dot{x}_1 & \dot{x}_2 \end{bmatrix}^T$$

$$A(t)=\begin{bmatrix} \boldsymbol{0} & \boldsymbol{I} \\ -\boldsymbol{M}^{-1}\boldsymbol{K} & -\boldsymbol{M}^{-1}\boldsymbol{C} \end{bmatrix}$$

$$\boldsymbol{B}=\frac{1}{M_2}[0 \quad 0 \quad 0 \quad 1]^T$$

$$\boldsymbol{U}(t)=F(t)$$

M, **K** and **C** are the system's mass, stiffness and damping matrices respectively, and have the form

$$\boldsymbol{M}=\begin{bmatrix} M_1 & 0 \\ 0 & M_2 \end{bmatrix} \quad \boldsymbol{K}=\begin{bmatrix} K(t)+K_1 & -K_1 \\ -K_1 & K_1 \end{bmatrix} \quad \boldsymbol{C}=\begin{bmatrix} C_1 & -C_1 \\ -C_1 & C_1+C_2 \end{bmatrix}$$

F(t) is the combination of the active control force and the uplift force, and the actuator is mounted between the frame and the base, as discussed in the previous section.

The objective of providing a constant contact force using an active pantograph can be described as the problem of designing an optimal control input to make the pantograph to track or follow a given reference state $\mathbf{X}_r(t)$. Here only one component of $\mathbf{X}_r(t)$should be tracked, that is the panhead displacement $x_{r1}(t)$ to keep the contact force constant. $x_{r1}(t)$ can be calculated through (7).

For an optimal tracking problem the performance measure can be defined as [12]

$$J=\frac{1}{2}\left[\boldsymbol{X}(t_f)-\boldsymbol{X}_r(t_f)\right]^T\boldsymbol{H}\left[\boldsymbol{X}(t_f)-\boldsymbol{X}_r(t_f)\right]$$

$$+\frac{1}{2}\int_{t_0}^{t_f}\left\{\left[\boldsymbol{X}(t)-\boldsymbol{X}_r(t)\right]^T\boldsymbol{Q}\left[\boldsymbol{X}(t)-\boldsymbol{X}_r(t)\right]+\boldsymbol{U}^T(t)\boldsymbol{R}\boldsymbol{U}(t)\right\}dt \qquad (22)$$

In the above equation, the time interval $[t_0, t_f]$, where t_0 and t_f are the beginning and the terminal times of the optimal control respectively, is generally defined to be longer than that of the external excitation, but this is not necessary for a periodically time-varying system if the reference state $\mathbf{X}_r(t)$ is also periodic. **H**, **Q** and **R** the weighting matrices whose magnitudes are assigned according to the relative importance attached to the state variables and to the control forces in the minimisation procedure of the performance measure. Because only the panhead displacement x_{r1} should be tracked and there is only one control force F(t), **H**, **Q** and **R** take the form

$$\boldsymbol{H}=\begin{bmatrix} h & & & \\ & 0 & & \\ & & 0 & \\ & & & 0 \end{bmatrix} \qquad \boldsymbol{Q}=\begin{bmatrix} q & & & \\ & 0 & & \\ & & 0 & \\ & & & 0 \end{bmatrix} \qquad \boldsymbol{R}=r \tag{23}$$

and

$$h,\ q,\ r>0$$

Then the optimal control force **U**(t) for maintaining a constant contact force has the form [13]

$$\boldsymbol{U}(t)=-\boldsymbol{R}^{-1}\boldsymbol{B}^{T}\boldsymbol{P}(t)\boldsymbol{X}(t)+\boldsymbol{R}^{-1}\boldsymbol{B}^{T}\boldsymbol{S}(t) \tag{24}$$

where **P**(t) and **S**(t) are the solutions of the following differential equations with their terminal conditions

$$\dot{\boldsymbol{P}}(t)=-\boldsymbol{A}^{T}(t)\boldsymbol{P}(t)-\boldsymbol{P}(t)\boldsymbol{A}^{T}(t)+\boldsymbol{P}(t)\boldsymbol{B}\boldsymbol{R}^{-1}\boldsymbol{B}^{T}\boldsymbol{P}(t)-\boldsymbol{Q} \tag{25a}$$

$$\boldsymbol{P}(t_f)=\boldsymbol{H} \tag{25b}$$

$$\dot{\boldsymbol{S}}(t)=-\left[\boldsymbol{A}^{T}(t)-\boldsymbol{P}(t)\boldsymbol{B}\boldsymbol{R}^{-1}\boldsymbol{B}^{T}\right]\boldsymbol{S}(t)-\boldsymbol{Q}\boldsymbol{X}_{r}(t) \tag{26a}$$

$$\boldsymbol{S}(t_f)=\boldsymbol{H}\boldsymbol{X}_{r}(t_f) \tag{26b}$$

Equations (25a,b) represent a matrix differential equation known as the Riccati equation and equations (26a,b) represent a vector differential equation.

It can be seen from (24) that the optimal control force is derived from feedback control (proportional to **X**(t)) and open-loop control (proportional to **S**(t)). The optimal feedback control gain matrix has the form

$$\boldsymbol{G}(t)=\boldsymbol{R}^{-1}\boldsymbol{B}^{T}\boldsymbol{P}(t)=\begin{bmatrix} g_1(t) & g_2(t) & g_3(t) & g_4(t) \end{bmatrix} \tag{27}$$

and the optimal open-loop control has the form

$$w(t)=\boldsymbol{R}^{-1}\boldsymbol{B}^{T}\boldsymbol{S}(t) \tag{28}$$

Thus the optimal control force can be written as

$$F(t)=-\boldsymbol{G}(t)\boldsymbol{X}(t)+w(t) \tag{30}$$

Fig. 13 shows simulations of the active pantograph which has the same parameters as discussed above and uses optimal control with optimal feedback coefficients $g_1(t)$,

$g_2(t)$, $g_3(t)$, $g_4(t)$ and the optimal open-loop control w(t). Comparing Fig. 13 (b) with Fig. 9 (d), it can be seen that similar results for both the contact force and the control force are achieved with both open-loop control and optimal control. Some important conclusions for the active pantograph using optimal control may be stated as follows:

1. Because the optimal control force is partly derived from feedback, this control strategy can resist external disturbances.

2. The optimal controller must know exactly where the panhead is in a span of the overhead wire because the control force includes open-loop control. Also the optimal feedback gain matrix is *periodically time-varying* with the same cycle as the stiffness fluctuation of the overhead wire.

3. The optimal control is based on full-state feedback, and this introduces possible measurement difficulties because accurate measurement of displacement and velocity can be difficult to achieve directly.

4 Conclusion

In the paper three control strategies to achieve a relatively constant contact force between an active pantograph and the overhead wire have been discussed. The advantages and disadvantages of the different control strategies have been highlighted. For the active pantograph under open-loop control there is no stability problem, but it also cannot respond to any external disturbances. The active pantograph using feedback control can respond to external disturbances, but it has a stability problem which is related to the pantograph itself and to the pantograph-catenary system. Thus a compromise between the stability and the performance has to be reached. The optimal control strategy can also resist external disturbances, and achieves the best theoretical performance. However, if the measurement problem is taken into account, its realisation is the most difficult. If the active pantograph under feedback control uses acceleration feedback alone, then it will be the least difficult to implement.

It has been mentioned above that the influence of the wave propagation in the overhead wire has not been included in the model. In addition, some factors such as initial sag of the overhead wire, excitation of the pantograph by the locomotive roof and aerodynamic forces should be investigated in the further studies.

5 References

[1] **Wu, T. X.** and **Brennan, M. J.** Analytical study of pantograph-catenary system dynamics. submitted to the Journal of Vehicle System Dynamics (1997).

[2] **Ockenden, J. R.** and **Taylor, A. B.** The dynamics of a current collection system for an electric locomotive. Proceedings of the Royal Society of London, Series A 322 (1971) pp. 447-468

[3] **Vinayagalingam, T.** Computer evaluation of controlled pantographs for current collection from simple catenary overhead equipment at high speed. ASME Journal of Dynamics Systems, Measurement, and Control, 105 (1983) pp. 287-294

[4] **Wormley, D. N. Seering, W. P. Eppinger, S. D.** and **O'Connor, D. N.** Dynamic performance characteristics of new configuration pantograph-catenary systems. Report No. DOT/OST/P34-85/023 US Department of Transportation, Oct. (1984)

[5] **Wu, T. X.** Study of current collection from catenary-pantograph at high speed by simulation. Journal of the Chinese Railway Society (in Chinese), 18 Aug. (1996) pp. 55-61

[6] **Yagi, T. Stensson, A.** and **Hardell, C.** Simulation and visualisation of the dynamic behaviour of an overhead power system with contact breaking. Vehicle System Dynamics, 25 (1996) pp. 31-49

[7] **Vinayagalingam, T.** Acceleration detection and inertia compensation of pantograph head using a constant flow hydraulic servo. ASME Journal of Engineering for Industry, 104 (1982) pp. 8-16

[8] **Galleotti, G. Galanti, M.** and **Magrini, S.** Servo actuated railway pantograph for

high-speed running with constant contact force. Proc. Instn. Mech. Engrs., Part F 207 (1993) pp. 37-49

[9] **Huber, D. Jörns, C.** and **Tessun, H.** Aktive Stromabnehmer bei Hochgeschwindigkeitszügen. Elektrische Bahnen 91 (1993) pp. 382-388

[10] **Thompson, A.** and **Davis, B.** An active pantograph with shaped frequency response employing linear output feedback control. Vehicle System Dynamics, 19 (1990) pp. 131-149

[11] **Lesser, M. Karlsson, L.** and **Drugge, L.** An interactive model of a pantograph-catenary system. Vehicle System Dynamics, Supplement 25 (1996) pp. 397-412

[12] **Meirovitch, L.** Dynamics and Control of Structures. (1990) John Wiley and Sons, New York

[13] **Sage, A. P.** and **White, C. C. III** Optimum System Control. 2nd edn (1977) Prentice-Hall, Englewood Cliffs

6 Figures

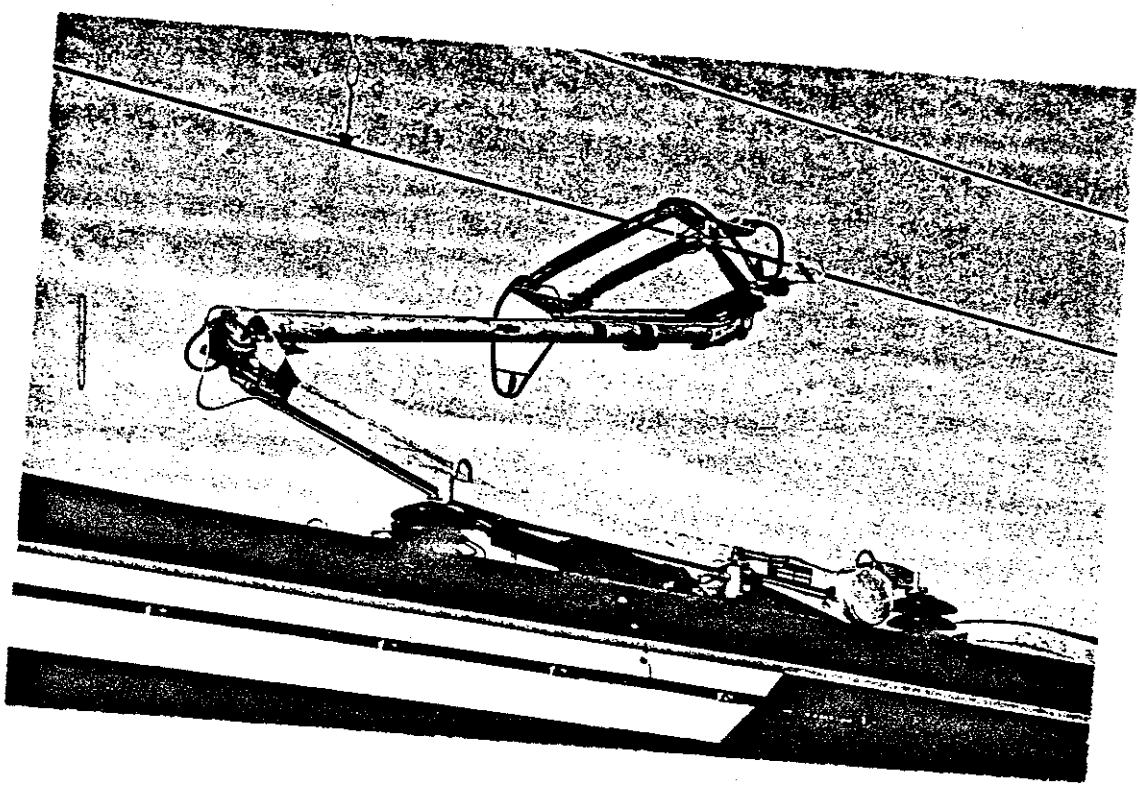

Fig. 1 A pantograph-catenary system in operation.

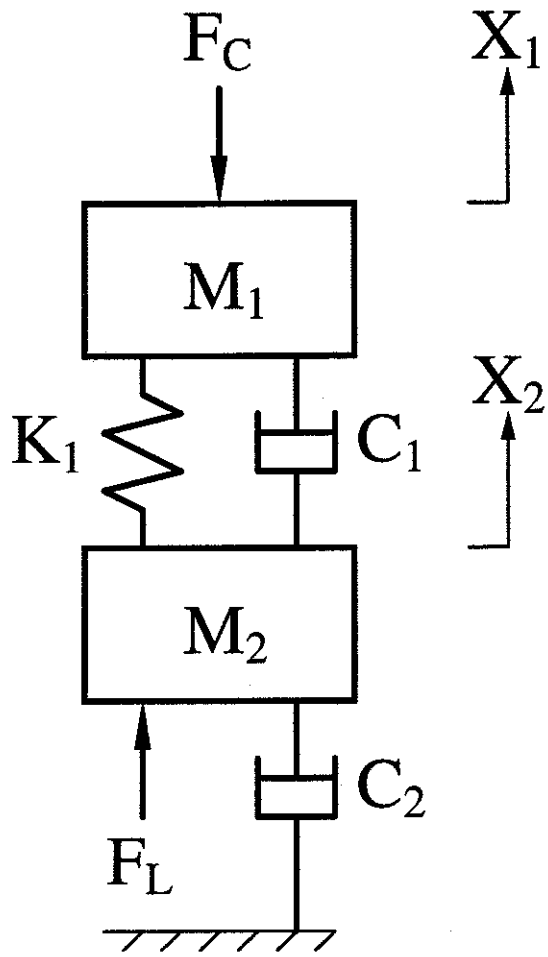

Fig. 2 Two DOF pantograph model.

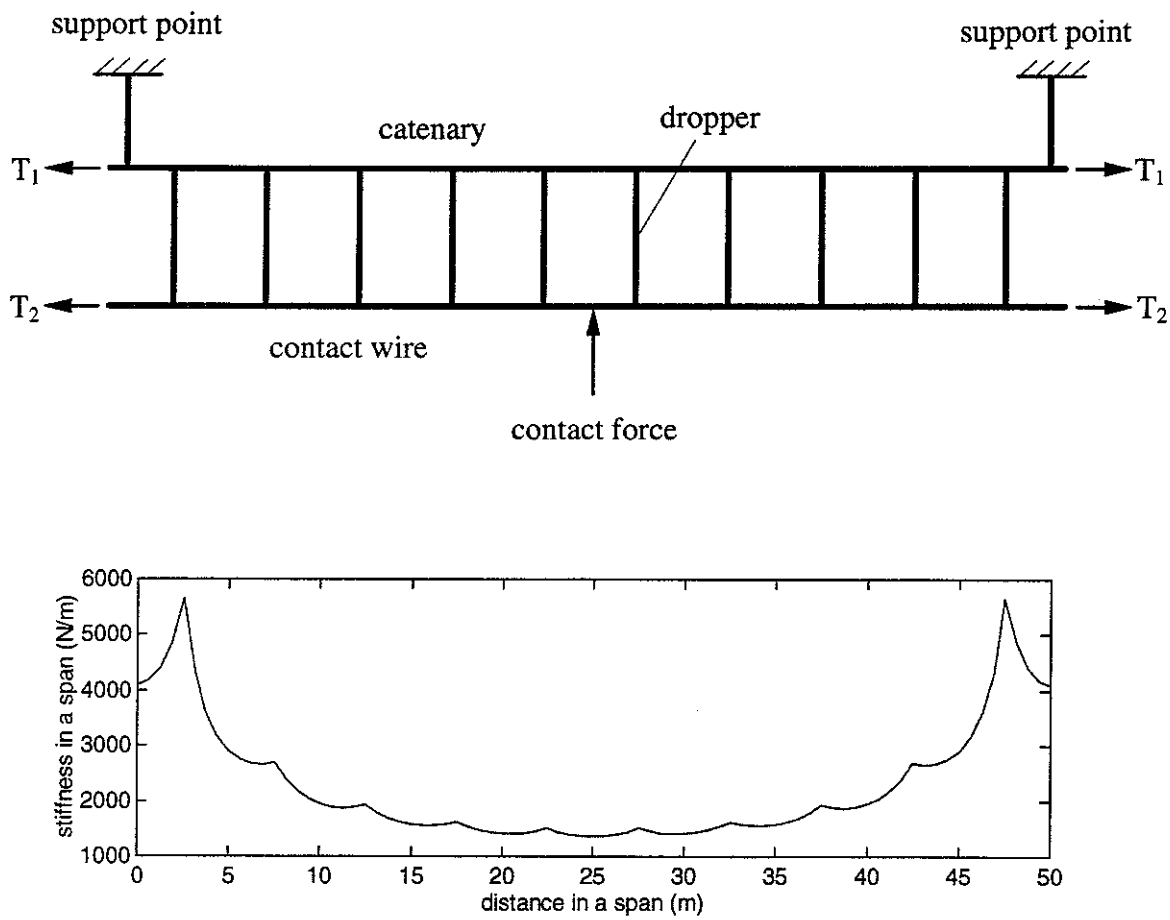

Fig. 3 A standard overhead wire system and the stiffness variation of the contact wire in a span, where T_1=T_2=9.8 kN.

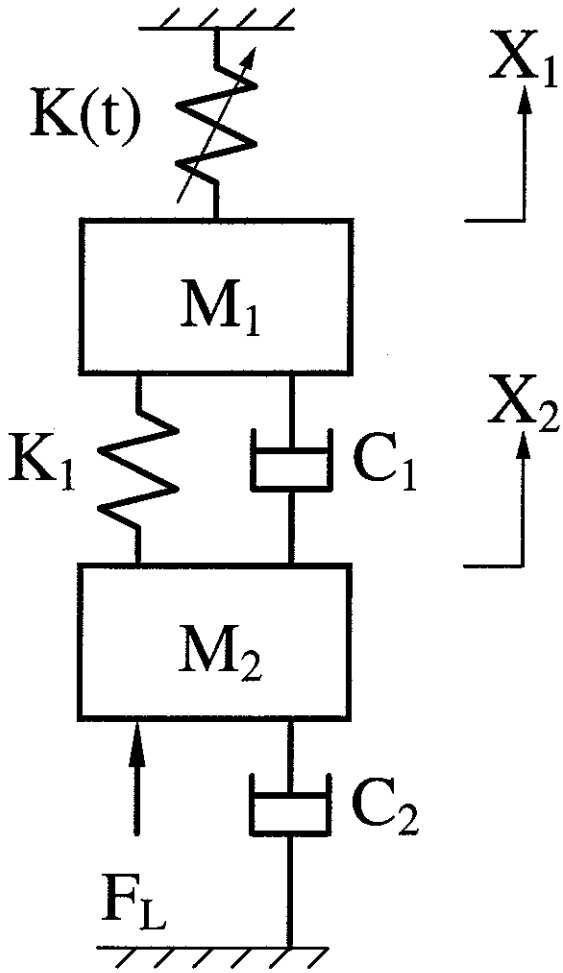

Fig. 4 The pantograph-catenary model considering the influence of the static stiffness variation of the overhead wire.

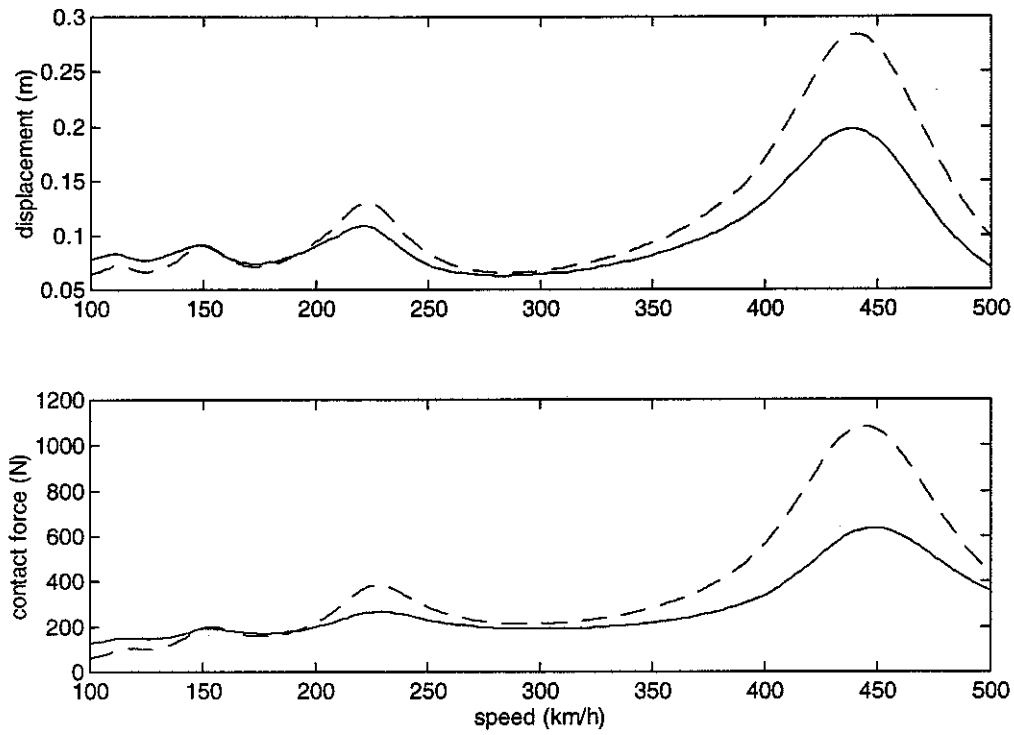

Fig. 5 Maximum (——) and peak-to-peak (- - - -) panhead displacement and contact force in the range of train's speed from 100 to 500 km/h.

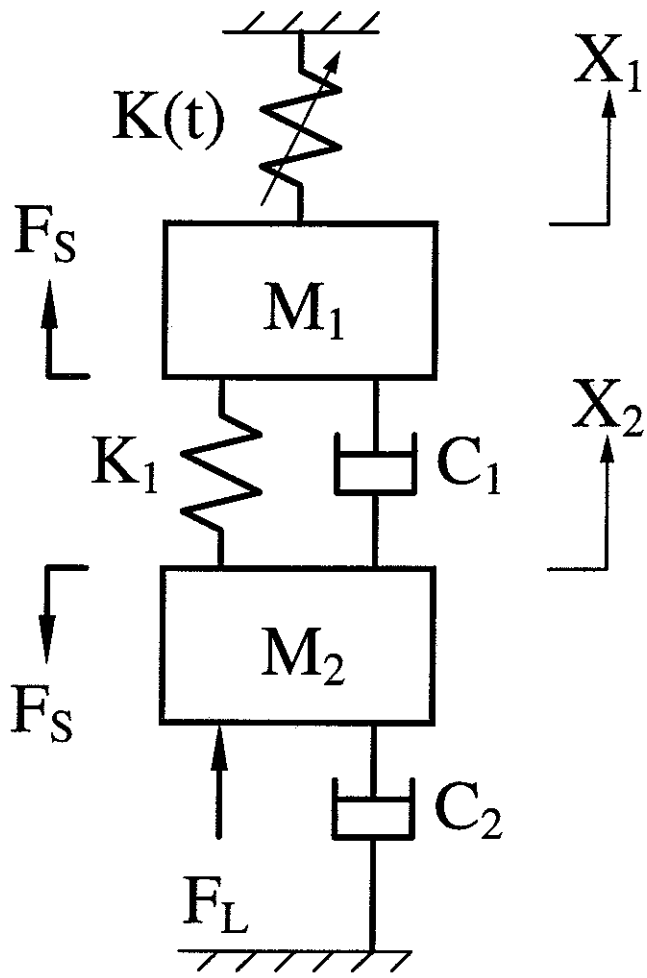

Fig. 6 The panhead-frame actuated active pantograph model.

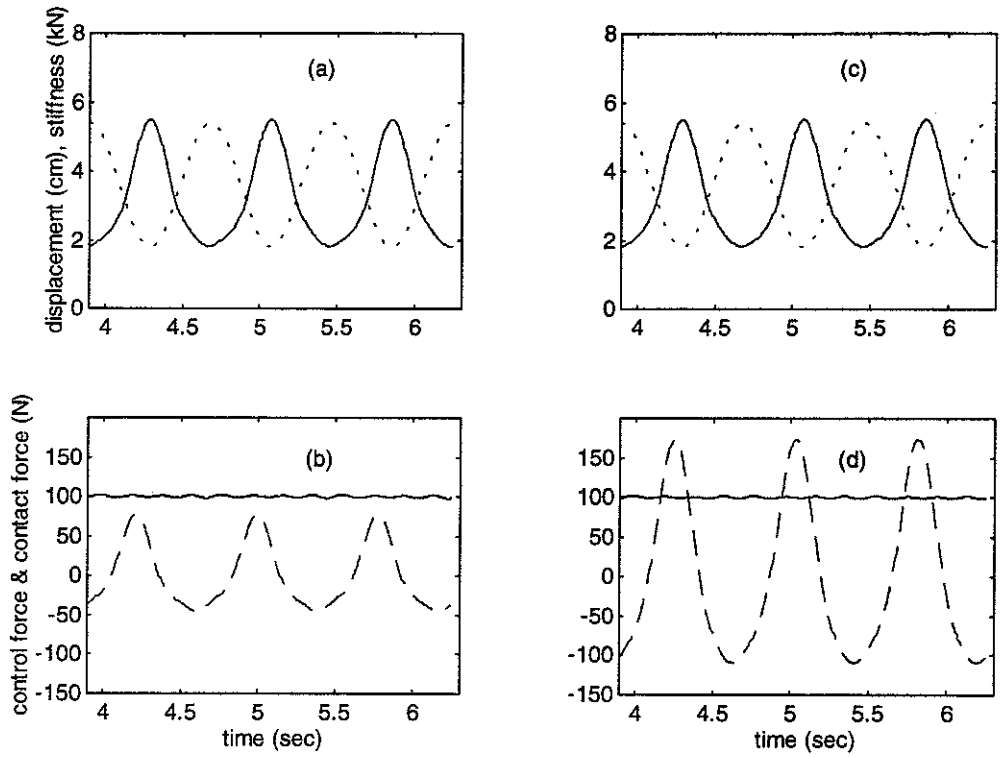

Fig. 7 Panhead displacement (——), contact force(——), open-loop control force(- - - -) and stiffness variation of overhead wire (·····). V=300 km/h, (a) and (b) for K_1=2kN/m, (c) and (d) for K_1=5kN/m.

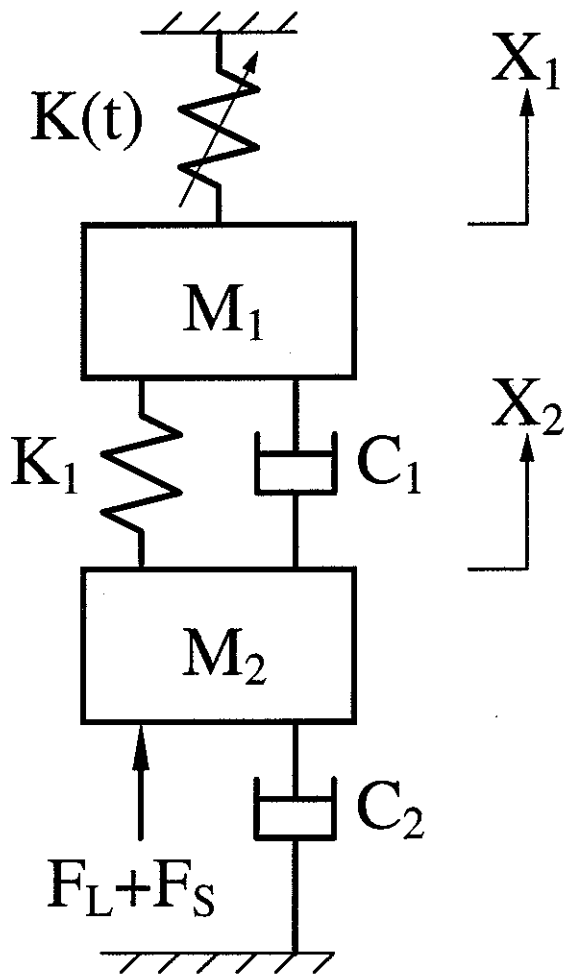

Fig. 8 The frame actuated active pantograph-catenary model.

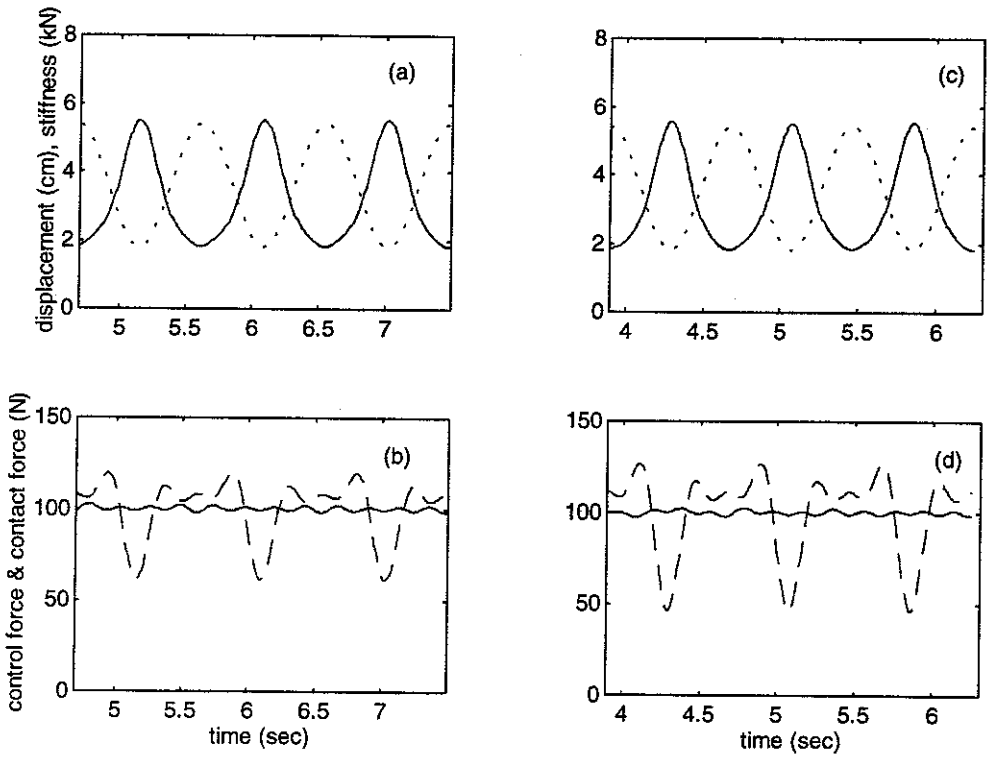

Fig. 9 Panhead displacement (——), contact force(——), open-loop control force including F_L(- - - -) and stiffness variation of overhead wire (·····). (a) and (b) for V=250 km/h, (c) and (d) for V=300 km/h.

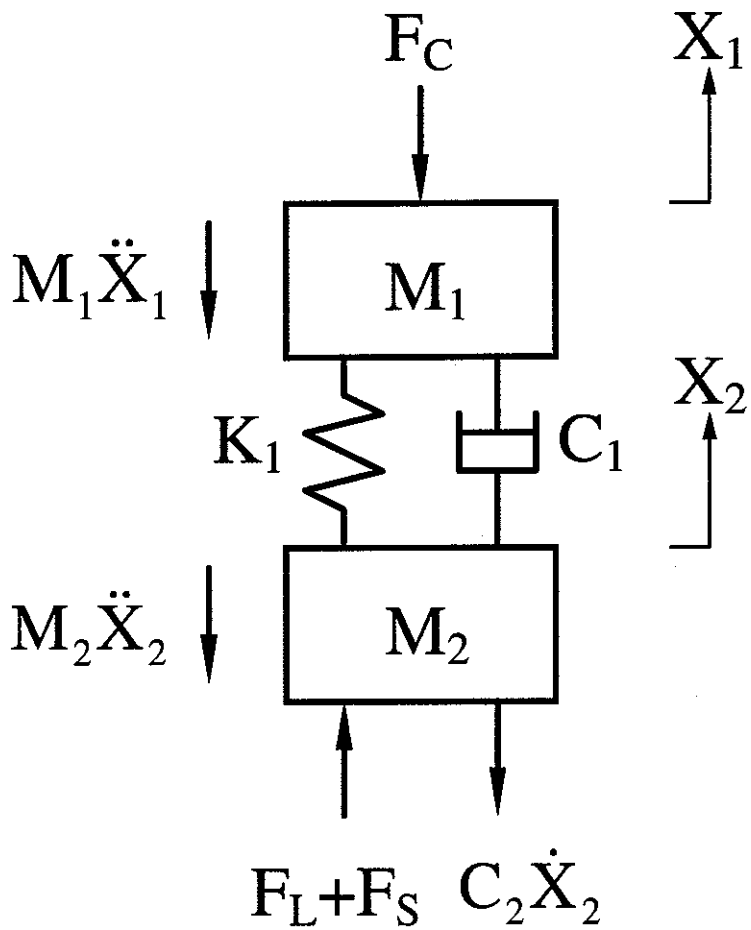

Fig.10 Isolated diagram of a frame actuated active pantograph.

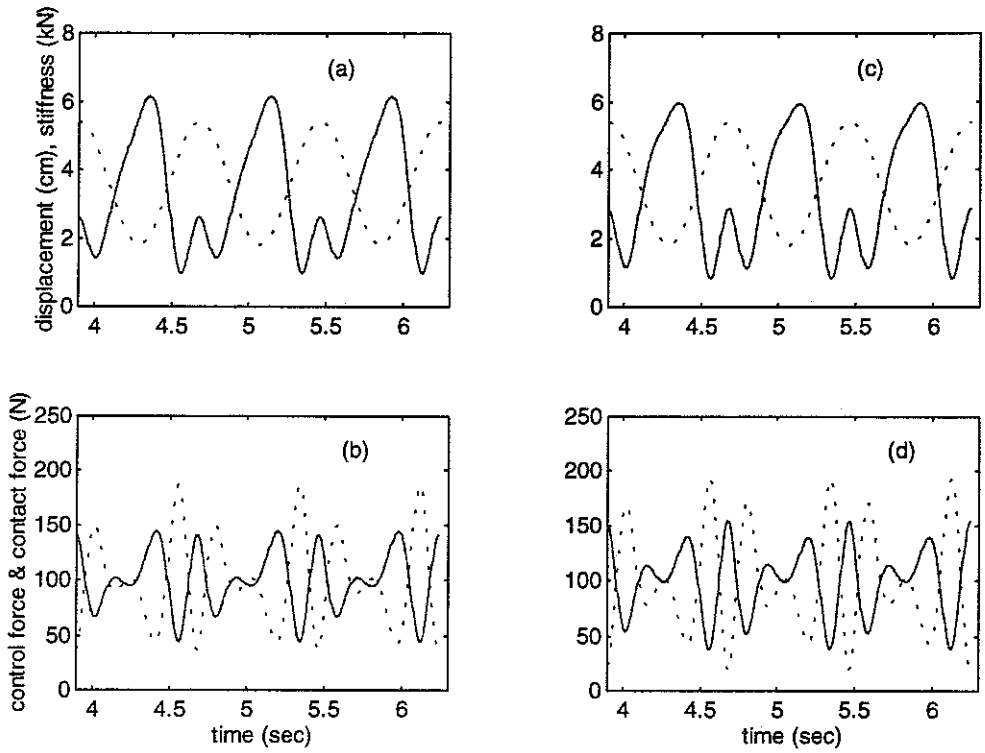

Fig.11 Panhead displacement (——), contact force(——), closed-loop control force including F_L (·····) and stiffness variation of overhead wire (·····). V=300 km/h, K_1=10kN/m, (a) and (b) for $g_1=g_2=0.6$, $g_3=0$, (c) and (d) for $g_1=g_2=0.6$, $g_3=0.5$.

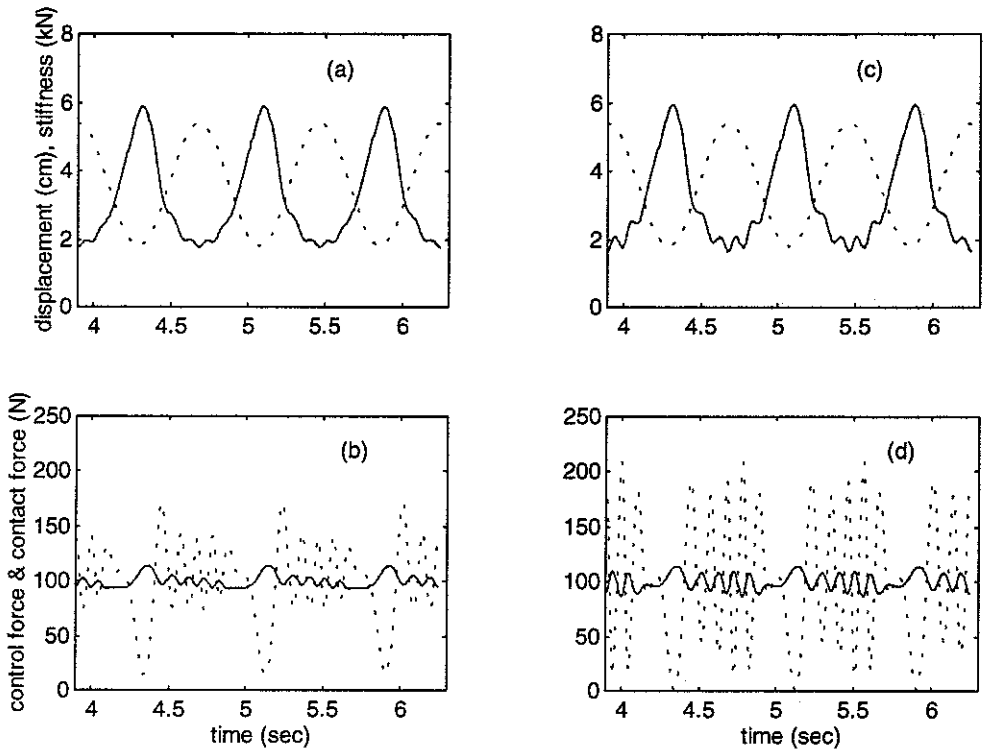

Fig.12 Panhead displacement (——), contact force(——), closed-loop control force including F_L (·····) and stiffness variation of overhead wire (·····). V=300 km/h, K_1=40kN/m, (a) and (b) for $g_1=g_2=0.9$, $g_3=0$, (c) and (d) for $g_1=g_2=0.9$, $g_3=0.3$.

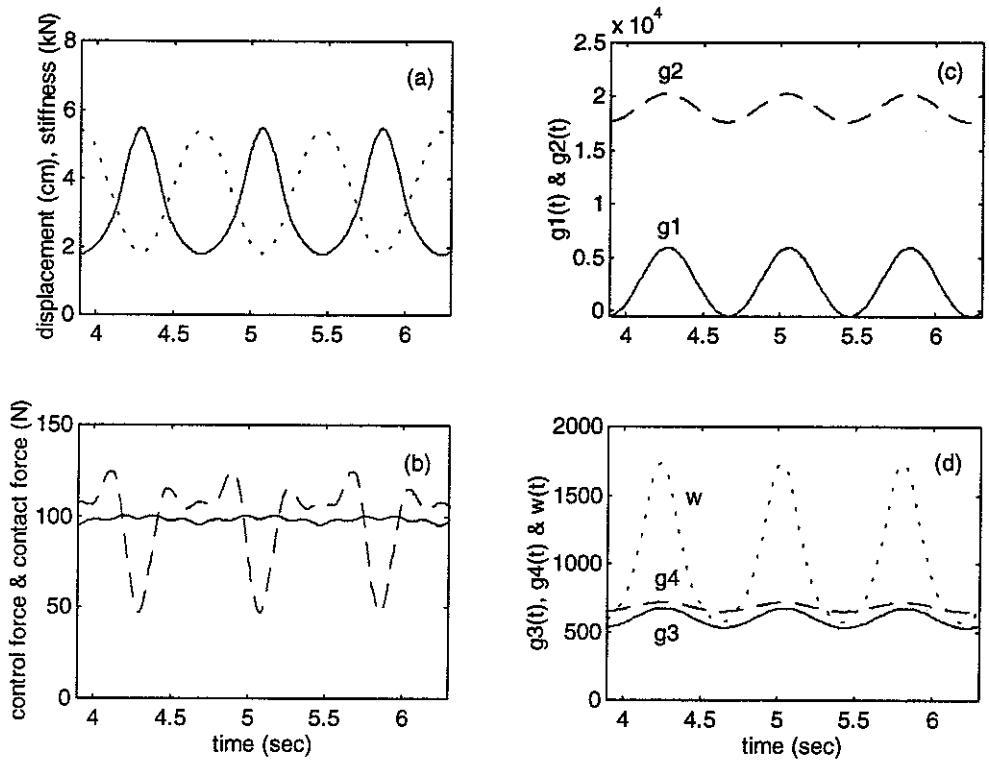

Fig.13 (a) and (b): panhead displacement (——), contact force(——), optimal control force (- - - -) and stiffness variation of overhead wire (·····). V=300km/h, h=10, $q=10^5$, $r=10^{-4}$. (c) and (d): optimal feedback coefficients $g_1(t)$, $g_2(t)$, $g_3(t)$, $g_4(t)$ and optimal open-loop control term w(t).